

## Bcl-2 Modulates Resveratrol-Induced ROS Production by Regulating Mitochondrial Respiration in Tumor Cells

Ivan Cherh Chiet Low,<sup>1,2</sup> Zhi Xiong Chen,<sup>1,2</sup> and Shazib Pervaiz<sup>1-4</sup>

### Abstract

Resveratrol is a naturally occurring flavanoid with potent apoptosis-inducing activity against human tumor cells. We investigated the effect of resveratrol on human leukemia cell lines, in particular its ability to induce intracellular reactive oxygen species production and the effect of Bcl-2 overexpression on this model. Exposure of CEM cells to increasing concentrations of resveratrol (0–50  $\mu$ M) resulted in an increase in mitochondrial superoxide production, decrease in transmembrane potential, and a concomitant decrease in cell viability. Whereas overexpression of Bcl-2 increased mitochondrial oxygen consumption and complex IV activity, CEM/Bcl-2 cells responded to the increased mitochondrial oxidative stress induced by resveratrol by significantly reducing mitochondrial respiration, complex IV activity, and  $O_2^-$  production, and promoted cell survival. The inhibitory effect of Bcl-2 on resveratrol-induced mitochondrial  $O_2^-$  production is further corroborated by the neutralization of this regulatory effect upon siRNA-mediated gene silencing of Bcl-2. These data provide evidence implicating mitochondrial metabolism in the anticancer activity of resveratrol, and underscore a novel regulatory role of Bcl-2 against exogenous oxidative stress through its ability to fine tune mitochondrial respiration, and by doing so maintaining mitochondrial  $O_2^-$  at a level optimal for survival. *Antioxid. Redox Signal.* 13, 807–819.

### Introduction

RESVERATROL (RSV) is a naturally occurring polyphenolic phytoalexin with diverse biological activity in a variety of disease models. Experimental evidence over the past couple of decades has established that, depending upon its concentration, RSV could have cytoprotective or cytotoxic effects on mammalian cells (26). These observations have provided the recent impetus to investigations into the molecular mechanisms and clinical potential of this flavanoid. To that end, our work and that of others have clearly highlighted the apoptosis-inducing effects of RSV in human tumor cells *in vitro* and *in vivo*, implicating a variety of cellular signaling networks (26). Interestingly, a significant number of earlier reports linked the various cellular effects of RSV to its ability to function as an antioxidant (12, 21, 25). However, this dogmatic view has been challenged by recent experimental evidence indicating that the compound at significantly higher concentrations is a strong inducer of intracellular reactive oxygen species (ROS) (6, 7, 17), and that some of the biological effects could be attributed to its pro- rather than antioxidant activity (2, 3, 32). This is particularly relevant to its death-

inducing activity on transformed or cancer cells; however, the underlying mechanism(s) of RSV-mediated ROS production remain undefined, despite some recent evidence implicating members of the NOX family (26).

A potent intracellular source of ROS is the mitochondrial electron transport chain, where the high probability of electrons leaking onto molecular oxygen ( $O_2$ ) favors the one electron reduction of  $O_2$  to superoxide anion ( $O_2^-$ ) (4). Considering the obligatory involvement of mitochondria in the execution of the intrinsic death pathway, excessive generation of ROS within the mitochondria could trigger oxidative modification of mitochondrial membrane lipids with a resultant change in mitochondrial outer membrane permeability and egress of pro-apoptotic proteins, such as cytochrome C, Smac/Diablo, and apoptosis-inducing factor (AIF). The permeabilization of mitochondria is a function of the balance between the pro-apoptotic and the anti-apoptotic members of the Bcl-2 family, whereby the former (Bax/Bak) upon translocation and oligomerization facilitate permeabilization and the latter (Bcl-2/Bcl-xL) stabilize mitochondrial membranes by inhibiting Bax/Bak oligomerization (1). Of note, involvement of intracellular ROS in the activation and mitochondrial

<sup>1</sup>Department of Physiology, Yong Loo Lin School of Medicine, and <sup>2</sup>NUS Graduate School for Integrative Sciences and Engineering, National University of Singapore, Singapore.

<sup>3</sup>Cancer and Stem Cell Biology Program, Duke-NUS Graduate Medical School, Singapore.

<sup>4</sup>Singapore-MIT Alliance, Singapore.

localization of Bax, as well as the ability of Bax to trigger mitochondrial ROS have been previously reported by our group and others (2). In addition, we recently demonstrated the effect of Bcl-2 overexpression on mitochondrial oxygen consumption, complex IV (cytochrome C oxidase; COX) activity, and  $O_2^-$  production in human cancer cells (8). These data provided evidence to link the pro-survival effect of Bcl-2 to a significant increase in mitochondrial respiration, COX activity, and  $O_2^-$  generation. Intriguingly, in the event of overt mitochondrial oxidative stress induced upon obstruction of the electron transport chain with antimycin A or glucose deprivation or hypoxia, Bcl-2 expression resulted in regulating mitochondrial respiration and COX activity to prevent deleterious accumulation of ROS and their effect on cell survival (8, 9).

Considering the essential role that the mitochondria plays in apoptotic execution as well as ROS generation, targeting mitochondria remains a major cornerstone of novel anticancer therapeutics and to that end, the aim of this study was to investigate the involvement of the mitochondria in RSV-induced ROS generation in tumor cells, and how that might be affected in cells harboring overexpression of the death inhibitory protein Bcl-2. Using human leukemia cells, we provide evidence that RSV induces dose-dependent increase in mitochondrial  $O_2^-$  production, which correlates with an increase in caspase 9 and 3 activity, a drop in mitochondrial transmembrane potential ( $\Delta\psi/m$ ), release of cytochrome C, and cell death. Of note, overexpression of Bcl-2 blunts the pro-apoptotic effect of RSV by regulating mitochondrial metabolism.

## Materials and Methods

### Cell lines and culture conditions

CEM human leukemia cells stably transfected with the control vector (CEM/Neo) or vector-containing human Bcl-2 (CEM/Bcl-2) were maintained in RPMI 1640 supplemented with 2 mM L-glutamine, 1% streptomycin-penicillin (v/v), 5% FBS (v/v) and 20  $\mu$ g/ml of G418 disulfate salt solution. HCT116 Wild Type and Bax/Bak<sup>-/-</sup> cell lines were generous gifts from Dr. Bert Vogelstein at Johns Hopkins University (Baltimore, MD). HCT116 cell lines were maintained in McCoy's5A (Invitrogen Life Technologies, Inc., Carlsbad, CA), supplemented with 10% fetal bovine serum, 1% L-glutamine, and 1% S-penicillin. Cells were subcultured in 75 cm<sup>2</sup> flasks every 3 days with a subculture ratio of 1:8 and maintained at 37°C in an incubator with humidified atmosphere of 95% air and 5% CO<sub>2</sub>.

### Determination of cell viability

Cell viability was determined by the MTT assay. In a typical assay,  $0.5 \times 10^5$  cells were mixed with 50  $\mu$ l of 4 mg/ml of 3-(4,5-dimethylthiazol-2-yl)-2,5-diphenyltetrazolium bromide (dissolved in RPMI-1640) in a 96-well format and incubated for 2 h at 37°C. After incubation, cells were centrifuged at 3000 rpm for 10 min, and the resultant formazan crystals were dissolved in a cocktail of 200  $\mu$ l DMSO and 10  $\mu$ l of Sorenson's glycine buffer (0.1 M glycine and 0.1 M NaCl, adjusted to pH 10.5). Cell viability was then quantified spectrophotometrically at an absorbance wavelength of 570 nm using a Spectrafluor Plus spectrophotometer (TECAN, GmbH, Grödig, Austria).

As the presence of N-acetyl cysteine (NAC) interferes with the MTT assay (14), cell viability was determined by the trypan blue dye exclusion test in all experiments involving NAC. Briefly,  $1 \times 10^6$  cells/ml were loaded with trypan blue dye on a hemocytometer slide at 1:1 (v/v) ratio. The number of cells was counted in all four quadrants under light microscope and the percentage of live cells was determined.

### Determination of caspases 3, 8 and 9 activities by enzymatic assay

Caspases 8, 9, and 3 activities were assayed using AFC-conjugated substrates (BioMol, Plymouth Meeting, MA). CEM/Neo and CEM/Bcl-2 ( $1 \times 10^6$ ) cells were plated in 12-well plates and immediately subjected to RSV treatment. Cells were harvested and washed with 1X PBS, resuspended in chilled cell lysis buffer (BD Pharmingen, San Diego, CA), and incubated on ice for 10 min. Subsequently, 50  $\mu$ l of 2X reaction buffer (10 mM HEPES, 2 mM EDTA, 10 mM KCl, 1.5 mM MgCl<sub>2</sub>, 10 mM DDT) and 1  $\mu$ l of the fluorogenic caspase-specific substrates (DEVD-AFC for caspase 3, LETD-AFC for caspase 8, and LEHD-AFC for caspase 9) were added to each sample and incubated at 37°C for 1 h. Protease activity was determined by measuring the relative fluorescence intensity at 505 nm with excitation at 400 nm using a Spectrafluor Plus spectrophotometer (TECAN, GmbH).

### Preparation of mitochondria-enriched fractions

Cells were harvested, washed once with ice-cold 1X PBS and pelleted by centrifugation at 1200 rpm for 5 min at 4°C. Pellet was resuspended in 10 volumes of buffer A (extraction buffer) containing a cocktail of protease inhibitors (1 mM PMSF, 1  $\mu$ g/ml leupeptin, 1  $\mu$ g/ml pepstatin, and 1  $\mu$ g/ml aprotinin) and incubated on ice for 20 min. After incubation, cells were homogenized with a manual homogenizer for 30 passages and then centrifuged at 300 g (4°C) for 10 min. The supernatant obtained was transferred into a new Eppendorf microcentrifuge tube and centrifuged at 13,000 g for 20 min at 4°C. The pellet consisted of intact mitochondria fraction, which was resuspended in mitochondrial medium II (200 mM mannitol, 100 mM sucrose, 0.1 mM EDTA, and 10 mM tris HCl adjusted to a pH of 7.4) and used immediately for oxygen consumption experiments.

### Measurement of mitochondrial oxygen consumption

Oxygen consumption of isolated mitochondria fraction obtained from  $1 \times 10^8$  cells was measured using the Oxytherm Electrode (Hansatech Instruments, Norfolk, UK). For the initiation of each measurement, the chamber was added with 1.25 ml of mitochondrial buffer III (200 mM mannitol, 75 mM sucrose, 0.1 mM EDTA, 10 mM K<sub>2</sub>HOP<sub>4</sub>, 10 mM KCl, and 10 mM Tris-HCl adjusted to pH 7.4) containing 10 mM succinate, 5  $\mu$ M rotenone, 80  $\mu$ M ATP, and 90  $\mu$ g of purified mitochondria. Oxygen consumption measurement was then initiated and monitored for 15 min at 30°C. To measure state 3 respiration, 0.2 mM ADP was added 5 min after initiation. Each measurement was initiated with 5 min of state 4 respiration, followed by another 10 min of state 3 respiration. Data acquisition and analysis were carried out using Oxygraph Plus software developed for high-resolution respirometry (Hansatech Instruments).

### Measurement of cytochrome c oxidase activity

Quantitative analysis of human complex IV or cytochrome c oxidase (COX) activity was performed using the Human Complex IV activity Microplate Assay Kit provided by MitoSciences (Eugene, OR). Experiments were carried out according to the protocol provided by the manufacturer.

### Detection of mitochondrial and intracellular ROS levels

Intra-mitochondrial  $O_2^-$  level was determined by MitoSOX Red (Invitrogen) staining and flow cytometric analysis. MitoSOX Red is a fluorescent probe that is highly sensitive to  $O_2^-$  oxidation. It is specifically targeted to the mitochondria, thus allowing the detection of mitochondrial specific  $O_2^-$  production (24). Approximately  $1 \times 10^6$  cells were pelleted and then resuspended with 100  $\mu$ l of plain RPMI-1640 containing 10  $\mu$ M MitoSOX Red reagent. Resuspended cells were then incubated for 15 min at 37°C, washed twice with 1X PBS, and resuspended again in fresh medium. Stained cells were immediately analyzed by flow cytometry (Beckman-Coulter Epics ALTRA flow cytometer) with excitation set at 510 nm and cell counter set at 10,000 events. Subsequent data analysis was performed using the WinMDI software.

Intracellular  $H_2O_2$  was assessed by flow cytometry with the fluorescent probe 2',7'-dichlorofluorescein diacetate (DCHF-DA, Molecular Probes, Invitrogen, Eugene, OR; 20  $\mu$ M), as described previously.

### Determination of mitochondrial transmembrane potential

Mitochondrial transmembrane potential ( $\Delta\Psi_m$ ) was measured by flow cytometry using the membrane potential sensitive dye, 3,3'-dihexyloxacarbocyanine iodide (DiOC<sub>6</sub>, Molecular Probes, 40 nM). Stained samples were immediately analyzed by flow cytometry (BD FACSCalibur, BD Biosciences, San Jose, CA) with excitation set at 488 nm (FL-1). All data were analyzed using the WinMDI software.

### Western blot analysis

Normalized protein samples were mixed with appropriate volumes of 5X loading buffer and heated at 100°C for 5 min. The samples were subjected to 12% (v/v) sodium dodecyl sulfate polyacrylamide gel electrophoresis (SDS-PAGE) at 100 V and 30 mA for about 2 h using the Bio-Rad Mini-PROTEAN 3 Cell (Hercules, CA). Resolved proteins were then transferred onto a polyvinylidene difluoride (PVDF) membrane by the semi-dry transfer method at 30 V and 270 mA for 45 min using the Hoefer™ TE 77 semi-dry transfer unit (Amersham Biosciences, Piscataway, NJ). The membrane was then blocked with 5% (w/v) fat-free milk in Tris-buffered saline containing 0.1% (v/v) Tween 20 (TBST) for 1 h with continuous rocking at 80 rpm. Excess milk was then washed off with TBST (3X 10 min). The membrane was subsequently probed for the protein of interest with the relevant primary antibody at 1:1000 dilution in TBST overnight at 4°C, together with gentle rocking. Unbound primary antibodies were washed off with TBST (3X 10 min) and probed again with the appropriate horseradish peroxidase (HRP)-conjugated secondary antibody at 1:5000 dilution in TBST containing 1% (w/v) fat-free milk for 1 h at room temperature (RT). The membrane was again subjected to three washes to remove excess secondary antibody before the

addition of HRP substrates (SuperSignal Chemiluminescent Substrate from Pierce, Rockford, IL). The desired proteins were next detected with Kodak Biomax MR X-ray film.

### siRNA-mediated gene silencing of Bcl-2

CEM/Bcl-2 cells were transfected with 50  $\mu$ M Bcl-2-specific siRNA (Ambion, Applied Biosystem, Carlsbad, CA) or scrambled siRNA using Oligofectamine™ reagent (Invitrogen) according to the manufacturer's protocol. Bcl-2 expression level was subsequently confirmed via Western blot assay as mentioned earlier.

### Purification of recombinant Bcl-2 proteins

*Escherichia coli* BL21 cells were transformed with GST-fusion construct containing the DNA of interest in 500 ml of LB medium with 100  $\mu$ g/ml of ampicillin and grown at 37°C overnight to reach OD<sub>600</sub>. The cultures were then induced with 0.4 mM of IPTG (isopropyl thio- $\beta$ -D-Galactoside) at 25°C for 6 h. Cells were subsequently harvested and resuspended in 50 ml buffer containing 50 mM Tris, pH 8.0, 150 mM NaCl, 1% Triton X-100, 1 mM DTT, 5 M EDTA, and 1 tablet of complete protease inhibitors cocktail (Boehringer, Ridgefield, CT). The cells were then sonicated on ice and centrifuged at 27,500 g for 10 min. The supernatant was then collected, added with 1 ml of glutathione sepharose resin (Amersham Biosciences, Sweden), and gently rocked on a shaker overnight at 4°C. Next, the beads with the bound proteins were packed in a column and washed with PBS for at least three times. In order to cleave GST tag from the recombinant proteins, 20 U/mL of thrombin protease (Amersham Biosciences) was added to the GST fusion protein still bound to the affinity column for 2 h at room temperature. The recombinant proteins were then eluted with high salt binding buffer with the Benzamide FF column connected in series with the affinity column as provided in the Amersham Biosciences GST purification Kit. The identity and purity of proteins was analyzed by SDS-PAGE and checked by Coomassie brilliant blue staining before being stored at -80°C.

### Transient transfection of pBabe-Bcl-2 plasmid

Transient transfection of HCT116WT and Bax/Bak<sup>-/-</sup> cells with Bcl-2 was performed using pBabe-Bcl-2 plasmids generously provided by Dr. Elizabeth Yang, Nashville, TN).  $2 \times 10^5$  cells were seeded in 6-well plates and transfected with Superfect Transfection Reagent™ (Qiagen, AR, Singapore) according to manufacturer's protocol. Cells were incubated in 2 ml of 10% McCoy's medium for 48 h before being harvested for further analysis.

### Measurement of superoxide dismutase activity

Quantitative analysis of superoxide dismutase (SOD) activity in isolated mitochondria was performed using the SOD activity Microplate Assay Kit provided by Assay Designs Inc. (Ann Arbor, MI). Mitochondria were isolated from  $10 \times 10^6$  cells per sample and subsequent experiment was carried out according to the protocol provided by the manufacturer.

### Statistical analysis

All experiments were performed at least three times and Student's *t*-test was used for obtaining significance when comparing data sets.

## Results

### *Bcl-2 alleviates RSV-induced mitochondrial $O_2^-$ production and cell death*

To investigate the effect of Bcl-2 expression on RSV-induced cell death, CEM/Neo and CEM/Bcl-2 cells were exposed to increasing concentrations of RSV (0–50  $\mu$ M) and cell viability was determined by the MTT assay. Results showed that overexpression of Bcl-2 endowed leukemia cells with a significant survival advantage, compared to the empty vector-transfected cells (Fig. 1A). To provide evidence that the growth inhibitory effect of RSV was a function of the execution of the apoptotic machinery, the activities of three major caspases (8, 9, and 3) were determined. A dose-dependent induction of caspase 8, 9, and 3 was detected in CEM/Neo

subjected to RSV treatment, while Bcl-2 overexpression significantly blunted the induction of caspase 9 and 3, but not caspase 8 (Figs. 1B, 1C, and 1D).

Furthering this,  $\Delta\Psi_m$ , cytosolic translocation of cytochrome C, and Bax/Bak oligomerization status were also determined to ascertain the involvement of the mitochondrial apoptotic pathway. Whereas, exposure of CEM/Neo cells to RSV resulted in a dose-dependent decrease in  $\Delta\Psi_m$  (Fig. 2B) and egress of cytochrome C (Fig. 2A), the overexpression of Bcl-2 significantly inhibited both, the effect of RSV on  $\Delta\Psi_m$  and cytochrome C release. Intriguingly, the activation of both Bax and Bak could not be detected in cell lysates following treatment with RSV (Fig. 2C), indicating the ability of RSV in triggering mitochondrial apoptotic execution independently of Bax/Bak activation. However, the ability of RSV to target

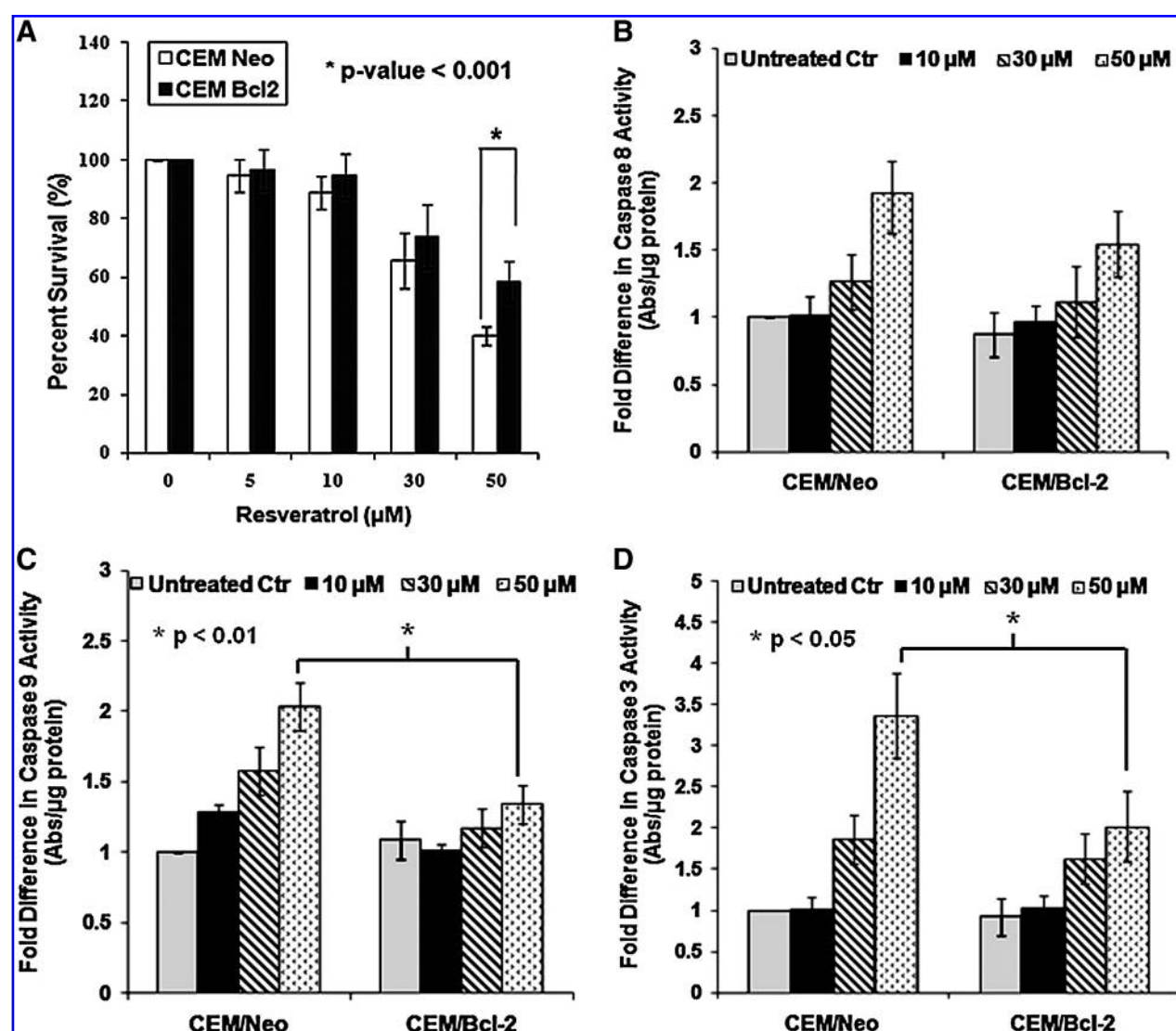


**FIG. 1.** Bcl-2 overexpression blocks RSV-induced apoptotic cell death. (A) CEM/Neo and CEM/Bcl-2 were treated with increasing concentrations of Trans-resveratrol (RSV; Sigma-Aldrich, MO) for 18 h and cell survival was assessed by the MTT assay as described in Materials and Methods. (B, C, and D) RSV-treated cells were harvested and assayed for caspase activity as described in Materials and Methods. Cells assayed for both caspase 8 and 9 activities were harvested at 6 h after RSV treatment while cells assayed for caspase 3 activity were harvested after 8 h of treatment. Data shown are Mean  $\pm$  SD of three independent experiments.

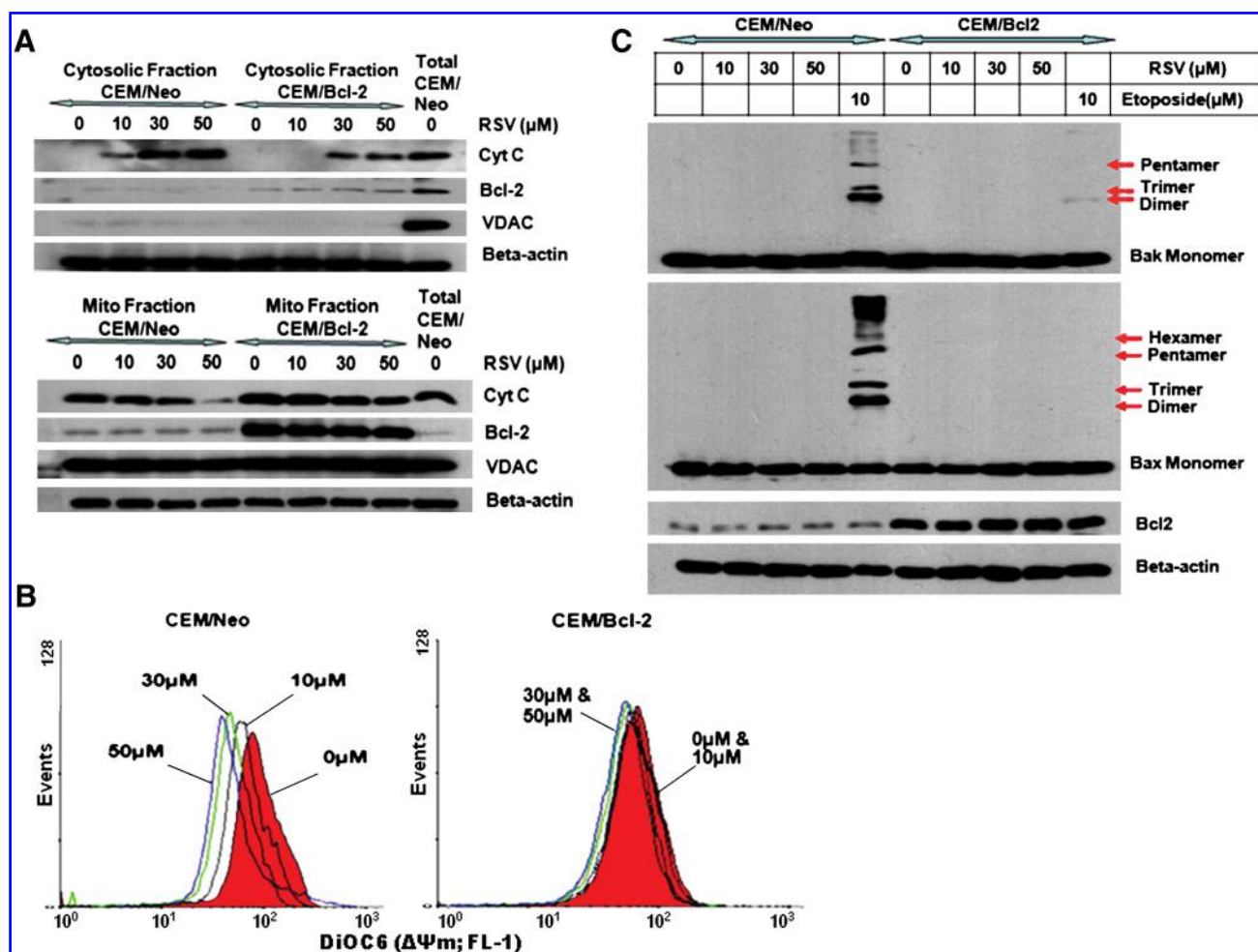


**FIG. 2. Bcl-2 overexpression inhibits RSV-induced mitochondrial apoptotic pathway.** (A) CEM/Neo and CEM/Bcl-2 cells were incubated with RSV (0–50  $\mu$ M) for 6 h, followed by Western blot analysis for cytochrome C and Bcl-2 in the cytosolic and mitochondrial fractions. VDAC expression was used as control for mitochondrial enrichment. (B) RSV-treated cells were loaded with the potential sensitive probe DiOC6 and  $\Delta\Psi_m$  was analyzed by flow cytometry, as described in Materials and Methods. (C) Bax and Bak oligomerization status in CEM cells was determined via Western blot analysis after 6 h of RSV treatment. Cell lysates were pre-incubated with cross-linking agent, bismaleimido-hexane (BMH from Thermo Scientific PIERCE, Rockford, IL), for 30 min at room temperature before being processed for Western blot analysis. 10  $\mu$ M etoposide was used as positive control for the oligomerization of Bax and Bak. (For interpretation of the references to color in this figure legend, the reader is referred to the web version of this article at [www.liebertonline.com/ars](http://www.liebertonline.com/ars)).

an alternative caspase 8-mediated cell death pathway that may function independently of the mitochondrial amplification loop could not be completely ruled out, as shown in our earlier communication (10).

Next, the effect of RSV on mitochondrial ROS production was assessed. Interestingly, kinetic analysis of mitochondrial  $O_2^-$  clearly indicated the ability of RSV to induce a dose-dependent increase in intra-mitochondrial  $O_2^-$  levels in CEM/Neo cells, which was significantly inhibited in CEM/Bcl-2 cells (Fig. 3A). These data were corroborated by *in vitro* study using isolated mitochondria with recombinant Bcl-2 protein (rBcl-2); pre-incubation of mitochondria isolated from CEM/Neo with rBcl-2 significantly inhibited the increase in RSV-induced mitochondrial  $O_2^-$  production, measured by Lucigenin-based chemiluminescence assay (Fig. 3B). These data correlated well with the cell viability data (Fig. 1A), strongly suggesting a link between RSV-induced mito-

chondrial  $O_2^-$  and its mitochondrial death-inducing effect. Intriguingly, despite being more resistant to RSV-induced oxidative stress, CEM/Bcl-2 cells consistently exhibited a mildly elevated level of basal mitochondrial  $O_2^-$  relative to its CEM/Neo counterpart (Fig. 3A). Indeed, this is in corroboration with our earlier report revealing a slight pro-oxidant state in CEM/Bcl-2 cells (8, 11).

Compared to the dose-dependent increase in mitochondrial  $O_2^-$  observed after 6 h of RSV treatment, mitochondrial  $O_2^-$  was highest in CEM cells treated with 10  $\mu$ M of RSV for 18 h, followed by a lower  $O_2^-$  level observed in cells treated with 30  $\mu$ M and 50  $\mu$ M RSV respectively (Figs. 3C and 3D). A kinetic analysis revealed that higher concentrations (30 and 50  $\mu$ M) triggered an initial burst of mitochondrial  $O_2^-$  in CEM cells, which gradually decreased over time (Fig. 3D). Of note, Bcl-2 overexpressing cells resisted the early (6 h) increase in mitochondrial  $O_2^-$  at lower concentrations of RSV (10  $\mu$ M),



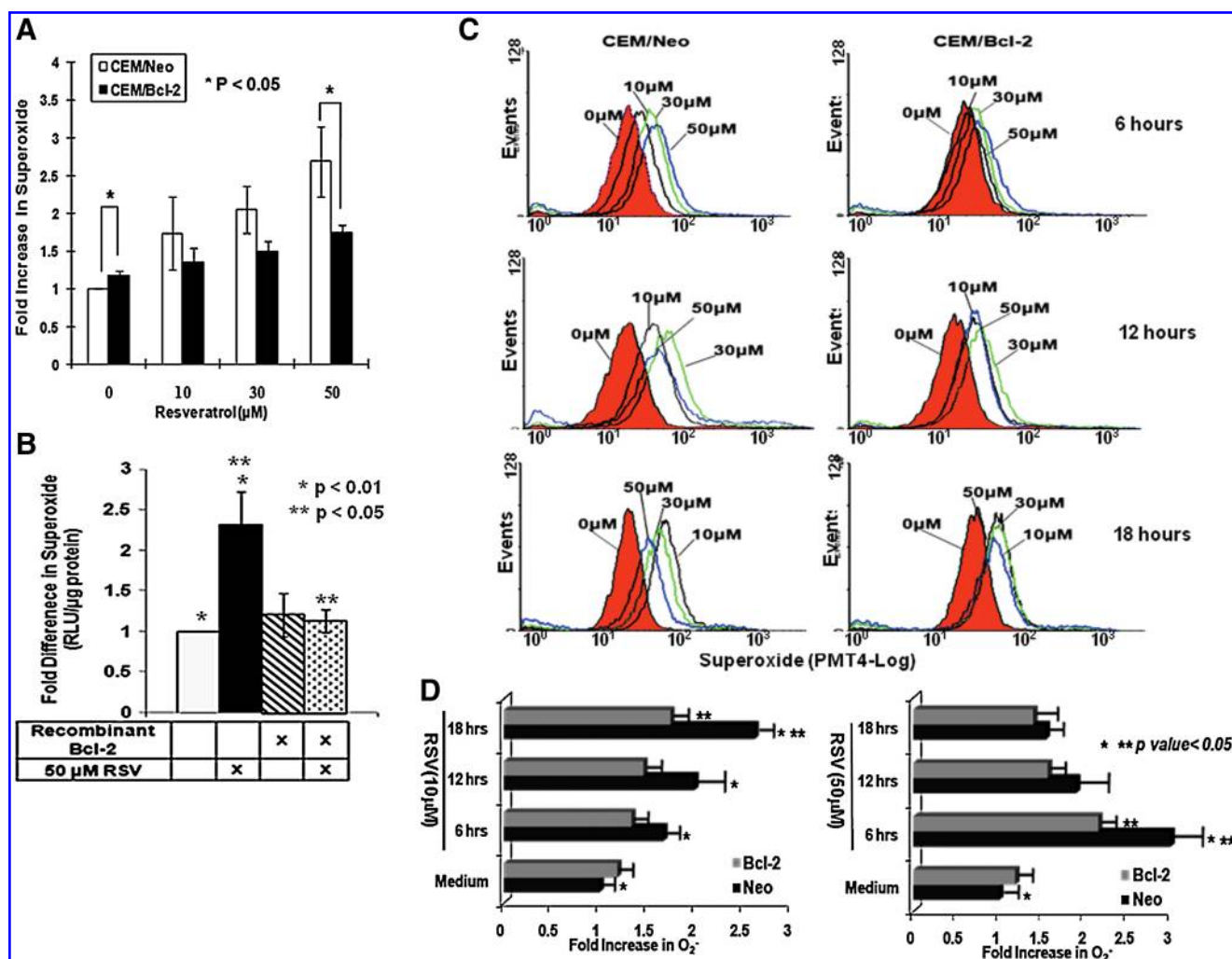


**FIG. 3. RSV induces mitochondrial  $O_2^-$  production in CEM cells, which is blocked by Bcl-2 expression.** (A) Intramitochondrial  $O_2^-$  level was measured in CEM/Neo and CEM/Bcl-2 following 6 h of RSV treatment by loading with MitoSOX RED and analyzed by flow cytometry using WinMDI software. Data shown are fold increase in G mean plotted in a graphical manner. (B) Mitochondria isolated from CEM/Neo cells were maintained in mitochondria medium II and were pre-incubated with 100 nM of recombinant Bcl-2 protein prior to 6 h incubation with 50  $\mu$ M RSV. Mitochondria were subsequently spun down and assayed for  $O_2^-$  production via a lucigenin-based chemiluminescence method. \* $p$  value represents mitochondria treated with RSV compared to nontreated mitochondria, whereas \*\* $p$  value is for the comparison of RSV-treated mitochondria pre-incubated with recombinant Bcl-2 prior to RSV treatment. (C) Kinetics (6, 12, and 18 h) of intramitochondrial  $O_2^-$  in CEM/Neo and CEM/Bcl-2 cells following exposure to various concentrations of RSV. Analysis for  $O_2^-$  was performed as in A. (D) Graphic representation of the differences in the kinetics of  $O_2^-$  production in CEM/Neo and CEM/Bcl-2 cells upon exposure to RSV. \* $p$  value represents CEM/Neo cells treated with RSV compared to nontreated cells (medium), whereas \*\* $p$  value is for CEM/Neo cells treated with RSV vs CEM/Bcl-2 cells treated similarly. All data shown are representative of three different experiments. (For interpretation of the references to color in this figure legend, the reader is referred to the web version of this article at [www.liebertonline.com/ars](http://www.liebertonline.com/ars)).

and even upon 12 and 18 h of exposure to RSV, the increase in  $O_2^-$  was significantly lower than in the mock transfected cells (Figs. 3C and 3D). These data provide strong support to the results shown in Figure 1 demonstrating RSV-mediated activation of the mitochondrial apoptotic pathway in CEM cells (Figs. 2A and 2B), thus indicating the involvement of a ROS-dependent mechanism inhibitable by Bcl-2 overexpression. As activation of the mitochondrial apoptotic pathway is expected to bring about the permeabilization of mitochondrial outer membrane and subsequent mitochondrial fragmentation (16, 33), not surprisingly RSV-induced apoptosis would be characterized by a drop in intracellular mitochondrial

content, with the observed reduction in mitochondrial  $O_2^-$  production upon high doses of RSV treatment being an obvious consequence.

#### Scavenging of $O_2^-$ , but not $H_2O_2$ , protects CEM cells from RSV-induced cell death

Despite being widely recognized as an antioxidant, RSV has been shown to exhibit pro-oxidant activity in several cell lines reported previously (3, 6, 32). Likewise, we report a similar burst in mitochondrial  $O_2^-$  in CEM cells upon RSV treatment. In order to elucidate whether this burst of  $O_2^-$  does

indeed play a role in RSV-induced cell death, we pretreated both CEM/Neo and CEM/Bcl-2 cell lines with SOD 1 h prior to RSV treatment. SOD enzyme's potent catalytic activity is responsible for the transmutation of  $O_2^-$  into  $H_2O_2$ . Pretreatment of both RSV-treated CEM/Neo and CEM/Bcl-2 cells with 50 and 100 units/ml SOD significantly protected the cells from RSV-induced cell death (Fig. 4A). In addition, a similar inhibitory effect of SOD (100 units/ml) was observed on RSV-induced cytochrome C release as well as on the activation of caspase 9 and 3 (Figs. 4B and 4C). However, it is of importance to note that this protection was absent in CEM cells pre-incubated with 200 units/ml SOD (Fig. 4A), possibly due to the overwhelming accumulation of intracellular  $H_2O_2$  in the cells as the conversion of  $O_2^-$  into  $H_2O_2$  increased. In order to further substantiate our reasoning, pre-incubation of RSV-treated CEM cells with 200 units/ml SOD concurrently with increasing doses of N-acetyl cysteine (NAC), a known scavenger of  $H_2O_2$ , restored the

viability of the cells to a level comparable to CEM cells pre-treated only with 100 units/ml of SOD (Supplemental Fig. 1A; see [www.liebertonline.com/ars](http://www.liebertonline.com/ars)). Nevertheless, pre-incubation of RSV-treated CEM cells with NAC alone did not yield any protection, suggesting that in the absence of SOD, only  $O_2^-$  but not  $H_2O_2$ , was responsible for the death-inducing effect of RSV. Taken together, these data suggest that the burst in  $O_2^-$  may be a potential trigger of RSV-induced cell death, while Bcl-2 overexpression ameliorates this death trigger by suppressing the production of mitochondrial  $O_2^-$  in these cells.

Furthering this, we monitored the level of intracellular  $H_2O_2$  in RSV-treated CEM cells across three different treatment time points via a flow cytometry-based method using DCHF-DA as the fluorescent probe. However, no detectable change in intracellular  $H_2O_2$  level was observed compared to exogenous addition of  $H_2O_2$  or the ROS inducing compound LY30 (27,31) used as positive controls (Fig. 5A). In addition,

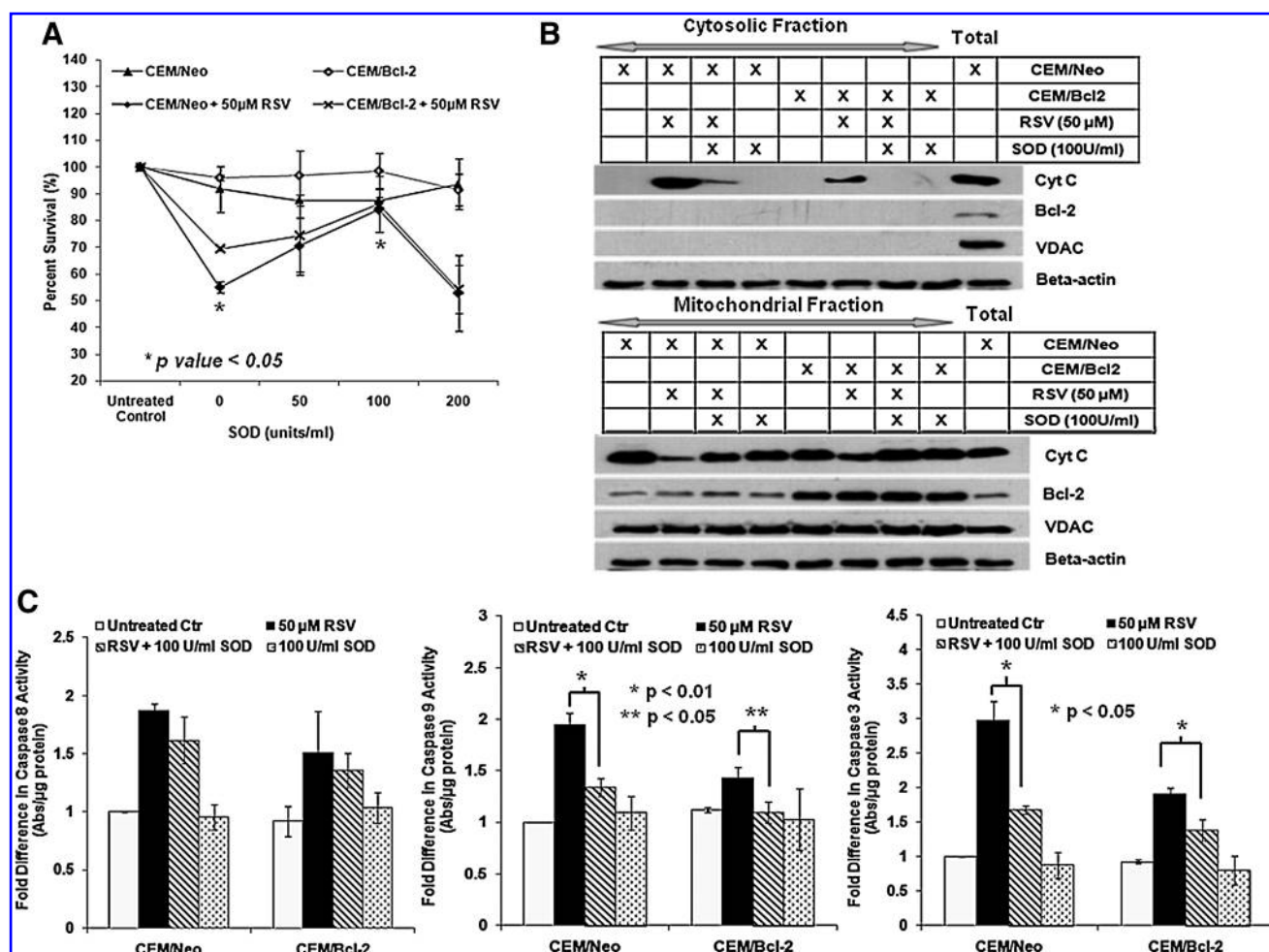


**FIG. 4.** Scavenging of  $O_2^-$  protects CEM cells from RSV-induced cell death. (A) MTT cell viability assay was performed on CEM/Neo and CEM/Bcl-2 cells following 18 h of RSV treatment. Cells were pre-incubated with increasing units of SOD (Sigma-Aldrich) for 1 h prior to RSV treatment. (B) RSV-treated (6 h) CEM cells were assayed for cytosolic translocation of cytochrome C after 1 h pre-incubation with 100 units/ml of SOD. Cytosolic and mitochondrial fractions were attained and processed for Western blot analysis, as described in Materials and Methods. VDAC expression was used as control for mitochondrial enrichment. (C) Activity of caspase 8, 9, and 3 of CEM/Neo and CEM/Bcl-2 cells were determined as described for Figure 1B. Cells were pre-incubated with 100 units/ml SOD for an hour prior to RSV treatment. Data shown are Mean  $\pm$  SD of at least three independent experiments.

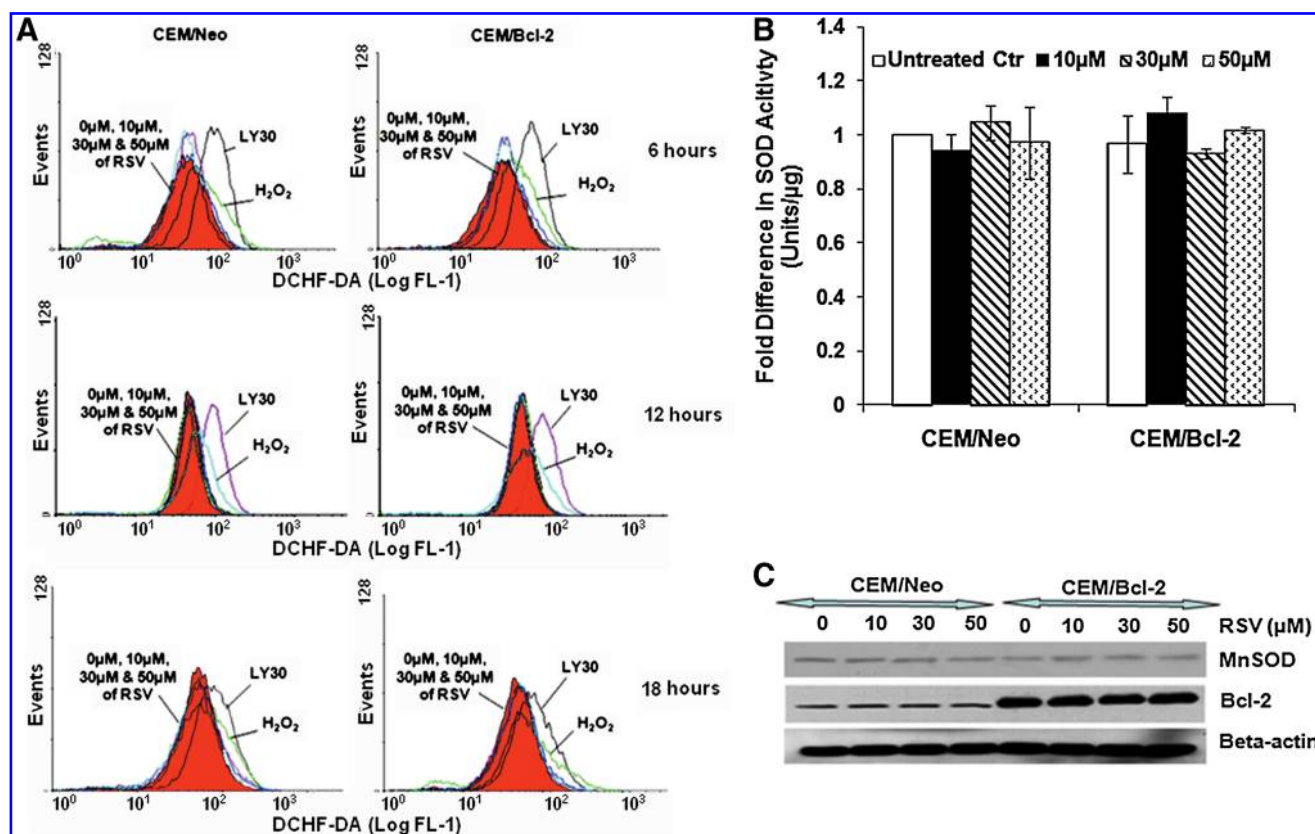


**FIG. 5. RSV-induced oxidative stress and cell death is independent of H<sub>2</sub>O<sub>2</sub> production.** (A) Flow cytometric analysis of intracellular H<sub>2</sub>O<sub>2</sub> in CEM/Neo and CEM/Bcl-2 via DCHF-DA staining. Samples were analyzed after 6, 12, and 18 h of RSV treatment, respectively. CEM cells treated with 1 h of 200 μM H<sub>2</sub>O<sub>2</sub> or 20 μM LY303511 (LY30) served as positive controls. (B) Mitochondria isolated from RSV-treated (18 h) CEM/Neo and CEM/Bcl-2 cells were assayed for SOD activity using a 96-well assay kit provided by Stressgen (Assay Designs Inc.). Data shown are Mean ± SD of at least three independent experiments. (C) Western blot analysis of MnSOD and Bcl-2 expressions in lysates from CEM/Neo and CEM/Bcl-2 cells following 18 h of incubation with RSV. β-actin was probed as a loading control. (For interpretation of the references to color in this figure legend, the reader is referred to the web version of this article at [www.liebertonline.com/ars](http://www.liebertonline.com/ars)).

SOD activity in isolated mitochondria and the expression of MnSOD, enzymes involved in the conversion of mitochondrial O<sub>2</sub><sup>-</sup> into H<sub>2</sub>O<sub>2</sub> (30), in both CEM/Neo and CEM/Bcl-2 was also analyzed after 18 h of RSV treatment. Despite numerous reports demonstrating the upregulation of MnSOD in response to oxidative stress (18, 28) as well as to chronic RSV treatment (29), no observable changes in mitochondrial SOD activity and MnSOD expression level was detected in both CEM/Neo and CEM/Bcl-2 following RSV treatment (Figs. 5B and 5C). These data point towards an H<sub>2</sub>O<sub>2</sub>-independent pathway of death execution activated upon exposure to RSV, but one that essentially requires the critical involvement of mitochondrial O<sub>2</sub><sup>-</sup>.

#### Downregulation of Bcl-2 sensitizes CEM/Bcl-2 cells to RSV-induced oxidative stress

In order to corroborate the results presented with cells stably expressing Bcl-2, gene silencing of Bcl-2 using Bcl-2 specific siRNA was performed in CEM/Bcl-2 cells, and the effect of RSV treatment on the redox status of these cells was investigated. Bcl-2 expression level was significantly reduced 48 h after transfection with Bcl-2-specific siRNA (Fig. 6A). Silencing of Bcl-2 triggered a considerable increase in mitochondrial O<sub>2</sub><sup>-</sup> production in RSV-treated CEM/Bcl-2 cells,

whereas mock-transfected CEM/Bcl-2 exhibited mitochondrial O<sub>2</sub><sup>-</sup> level similar to that of nontransfected CEM/Bcl-2 cells (Fig. 6B). Here, reduction in Bcl-2 expression in CEM/Bcl-2 paralleled an increase in RSV-induced mitochondrial O<sub>2</sub><sup>-</sup> production, thus indicating that Bcl-2 overexpression was indeed responsible for the protection of CEM/Bcl-2 against RSV-mediated oxidative stress.

#### Bcl-2 alleviates RSV-induced cell death and mitochondrial superoxide production in HCT116 wild-type and Bax/Bak double knockout cells

With numerous reports demonstrating the elevation of ROS production downstream of Bax/Bak-mediated mitochondrial membrane permeability transition (MPT) (19, 20), it appears plausible that protection by Bcl-2 against RSV-induced mitochondrial O<sub>2</sub><sup>-</sup> production may simply be secondary to its ability to inhibit Bax/Bak oligomerization and its associated release of mitochondrial ROS. Therefore, we proceeded to investigate the effect of Bcl-2 overexpression on the viability and mitochondrial redox status of RSV-treated HCT116 wild-type (HCTWT) and HCT116 double knockout (HCTDKO) cells. Interestingly, RSV was equally effective in the killing of both HCTWT and HCTDKO cells, albeit the requirement of a higher killing dose



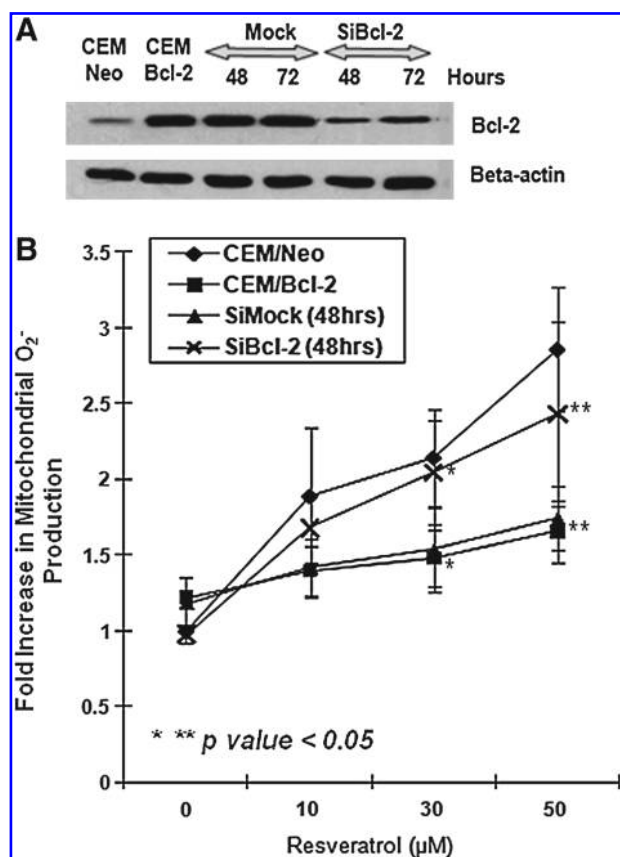


**FIG. 6. Knockdown of Bcl-2 increases RSV-induced mitochondrial O<sub>2</sub><sup>-</sup> production in CEM/Bcl-2 cells.** (A) Bcl-2 gene knockdown was performed in CEM/Bcl-2 cells by transfection with Bcl-2 specific siRNA. Lysates from cells following transfection for 48 h and 72 h were assessed for Bcl-2 expression by Western blot analysis. (B) Intramitochondrial O<sub>2</sub><sup>-</sup> was detected in cells transfected siBcl-2 by loading with the fluorescent probe, MitoSOX RED. Cells were then treated with 6 h of RSV before being subjected for further analysis. siMock represents CEM/Bcl-2 cells transfected with non-specific scrambled siRNA. Data shown are Mean  $\pm$  SD of at least three independent experiments. \**p* value represents the difference between CEM/Bcl-2 and siBcl-2 cells following treatment with 30  $\mu$ M RSV, whereas \*\**p* value represents the difference between CEM/Bcl-2 and siBcl-2 cells following treatment with 50  $\mu$ M RSV.

as compared to CEM cells (Fig. 7A). In addition, the absence of Bax and Bak appeared to have little effect on RSV-induced mitochondrial O<sub>2</sub><sup>-</sup> production in HCT116 cells (Fig. 7D). Importantly, Bcl-2 overexpression, as compared to its empty vector transfected counterpart, clearly protected HCT116 cells against RSV-induced cell death and mitochondrial O<sub>2</sub><sup>-</sup> production, even in the absence of Bax and Bak (Figs. 7B–7D). These findings clearly indicate the ability of Bcl-2 in the regulation RSV-induced mitochondrial O<sub>2</sub><sup>-</sup> in a manner independent of Bax and Bak activation.

#### Homeostatic regulation of mitochondrial respiration in CEM/Bcl-2 protects against RSV-induced oxidative stress

Spurred by our recent reports demonstrating a possible regulatory link between Bcl-2 and the mitochondrial respira-

tory system (8), oxygen consumption studies were performed on mitochondria isolated from RSV-treated CEM/Neo and CEM/Bcl-2 cells. 50  $\mu$ M of RSV was specifically selected as the preferred treatment dose since the protection conferred by Bcl-2 overexpression was previously observed to be most significant at this particular dose (Fig. 1A). Here, succinate-driven mitochondria respiration was clearly higher in CEM/Bcl-2 compared to CEM/Neo (Fig. 8A). This is in agreement with our postulated model that Bcl-2, being able to engage the mitochondrial respiratory chain, enhances the basal mitochondrial respiratory activity of the cells and thus generates a mild pro-oxidant state that confers the cells with a survival advantage (8, 11). More importantly, 6 h of 50  $\mu$ M RSV treatment triggered a drop in mitochondrial respiration in CEM/Bcl-2 but not in CEM/Neo (Figs. 8B and 8C), whereby oxygen consumption rate in CEM/Bcl-2 was brought down to a level comparable to that of CEM/Neo (Fig. 8D). It is important to note that the higher oxygen consumption rate observed in untreated CEM/Bcl-2 is not a result of an increase in uncoupled respiration as determined by the higher respiratory control ratio (RCR) seen in untreated CEM/Bcl-2 cells (Fig. 8E).

Likewise, evaluation of COX activity revealed corresponding observations to that of the oxygen consumption profile of RSV-treated CEM cells. Corroborating our earlier report (8), basal COX activity in CEM/Bcl-2 was significantly higher than that of CEM/Neo (Figs. 8F and 8G). However, a dose-dependent decline in COX activity was observed in CEM/Bcl-2 cells upon RSV treatment, with COX activity being reduced to a level comparable to that of CEM/Neo cells (Fig. 8F). In addition, silencing of Bcl-2 decreased COX activity in CEM/Bcl-2 to a level similar to that of CEM/Neo, whereas RSV-treatment did not alter the activity of COX in Bcl-2 silenced CEM/Bcl-2 cells (Fig. 8G). Of note, neither overexpression of Bcl-2 nor RSV-treatment affected the expression level of COX subunit I (Fig. 8H), indicating that the observed changes in COX activity was not an effect of a change in COX expression status.

## Discussion

We provide evidence that overexpression of Bcl-2 endows cancer cells the ability to downregulate COX activity in response to increasing oxidative stress triggered by RSV treatment. Reduction in COX activity is likely to reduce the flow of electrons across the ETC, with the concomitant decrease in mitochondrial O<sub>2</sub><sup>-</sup> by-production being the end result. Therefore, Bcl-2 appears to function as a brake in the mitochondrial respiratory system, preventing the accumulation of RSV-induced mitochondrial O<sub>2</sub><sup>-</sup> before it reaches a level catastrophic to the cell. Indeed, these findings corroborate our recent findings on the regulatory activity of Bcl-2 on mitochondrial oxygen consumption and COX activity. This allows the tumor cell to adjust the ETC activities according to its mitochondrial redox status, thereby facilitating the maintenance of intracellular ROS at a level optimal for cell survival upon stress triggers.

Our study highlighted the biphasic nature of O<sub>2</sub><sup>-</sup> as a signaling molecule in the regulation of cell death and proliferation. As shown in our earlier report, a mild increase in intracellular O<sub>2</sub><sup>-</sup> induced by low concentrations of RSV generates a slight pro-oxidant milieu that favors cell survival

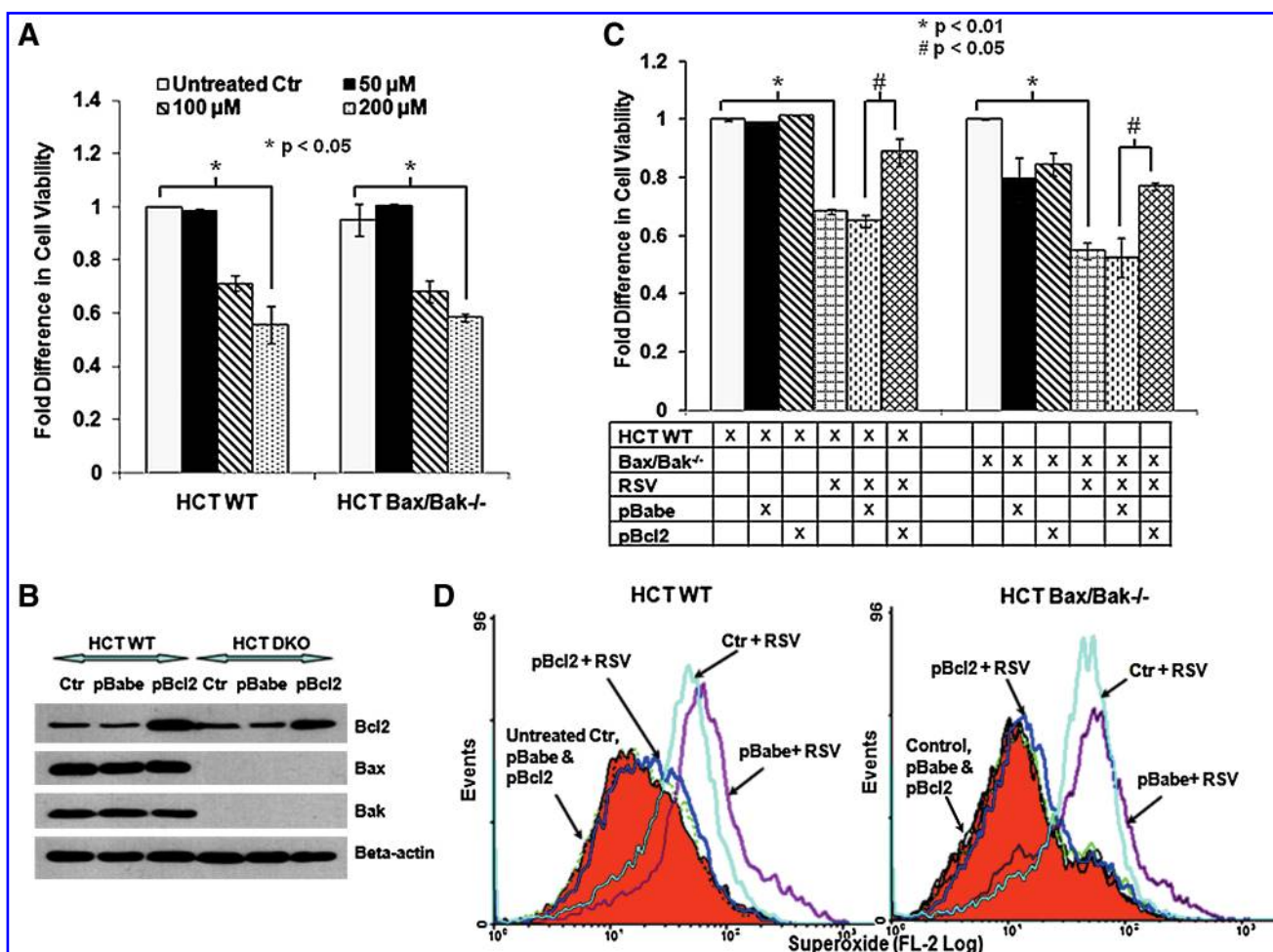


**FIG. 7.** Bcl-2 overexpression protects against RSV-induced oxidative stress and cell death independent of Bax and Bak. (A) HCT116 Wild Type (HCTWT) and HCT116 Bax and Bak Double Knock Out (HCT Bak/Bak<sup>-/-</sup>) cells were treated with increasing doses of RSV (50–200  $\mu$ M) for 24 h before being harvested and assessed for cell viability via MTT assay, as described in previous section. (B) Bcl-2 transfection of HCTWT and DKO was performed using Superfect Transfection Reagent (Qiagen) as described by manufacturer's protocol. pBabe plasmid were used as empty vector control and cells were harvested 48 h after transfection. (C) pBcl-2 transfected HCTWT and DKO cells were treated with 200  $\mu$ M RSV for 24 h before being harvested for cell viability assay as described in A. Data shown are Mean  $\pm$  SD of at least three independent experiments. (D) pBcl-2 transfected HCTWT and DKO cells were treated with 200  $\mu$ M RSV for 6 h before being harvested for mitochondrial O<sub>2</sub><sup>-</sup> measurement via FACS analysis using MitoSOX Red dye. All data were analyzed using WinMDI software. (For interpretation of the references to color in this figure legend, the reader is referred to the web version of this article at [www.liebertonline.com/ars](http://www.liebertonline.com/ars)).

(2, 3), while here we provide evidence that relatively higher concentrations of RSV stimulated mitochondrial O<sub>2</sub><sup>-</sup> production, and contributed to the death-inducing effect of RSV. Though the NADPH oxidase (Nox) family has been implicated as the primary source of RSV-induced cytosolic O<sub>2</sub><sup>-</sup> (2, 3), the precise source of RSV-induced mitochondrial O<sub>2</sub><sup>-</sup> remains uncertain. Previous studies suggest that the involvement of transition metal ions as the catalyst of electron transfer from RSV to oxygen molecules in the mitochondria (6, 7) may be a possible mechanism that accounts for the increase in mitochondrial O<sub>2</sub><sup>-</sup> observed in RSV-treated CEM cells.

Importantly, Bcl-2 overexpression significantly protected CEM cells from the deleterious effects of RSV-induced oxidative stress, possibly through downregulation of COX activity and the resultant decrease in respiration-dependent O<sub>2</sub><sup>-</sup> production. Indeed, our results suggest that the protection conferred by Bcl-2 overexpression against RSV-induced cell death may be partially attributed to its regulatory capacity on

mitochondrial ROS production. Therefore, we propose that Bcl-2 overexpression empowers cells to modulate their mitochondrial respiratory profile, adjusting intracellular ROS to nondetrimental levels even in the presence of ROS inducers such as antimycin A and RSV (8). Although it was previously suggested that the reinforcement of the antioxidant defenses observed in Bcl-2 overexpressing cells may be a compensatory response to the chronic mild pro-oxidant state (15), we postulate that the involvement of antioxidant enzymes in the defense against RSV-induced mitochondrial oxidative burst in our system is, at best, minimal. This is because the expression level of MnSOD, the primary SOD isoform responsible for the scavenging of mitochondrial O<sub>2</sub><sup>-</sup> (30), was comparable between CEM/Neo and CEM/Bcl-2 cells (Fig. 5C). In fact, the poor response of MnSOD against RSV-induced oxidative stress in CEM cells further accentuates the significance of our model as part of the mitochondrial antioxidant defense machinery.

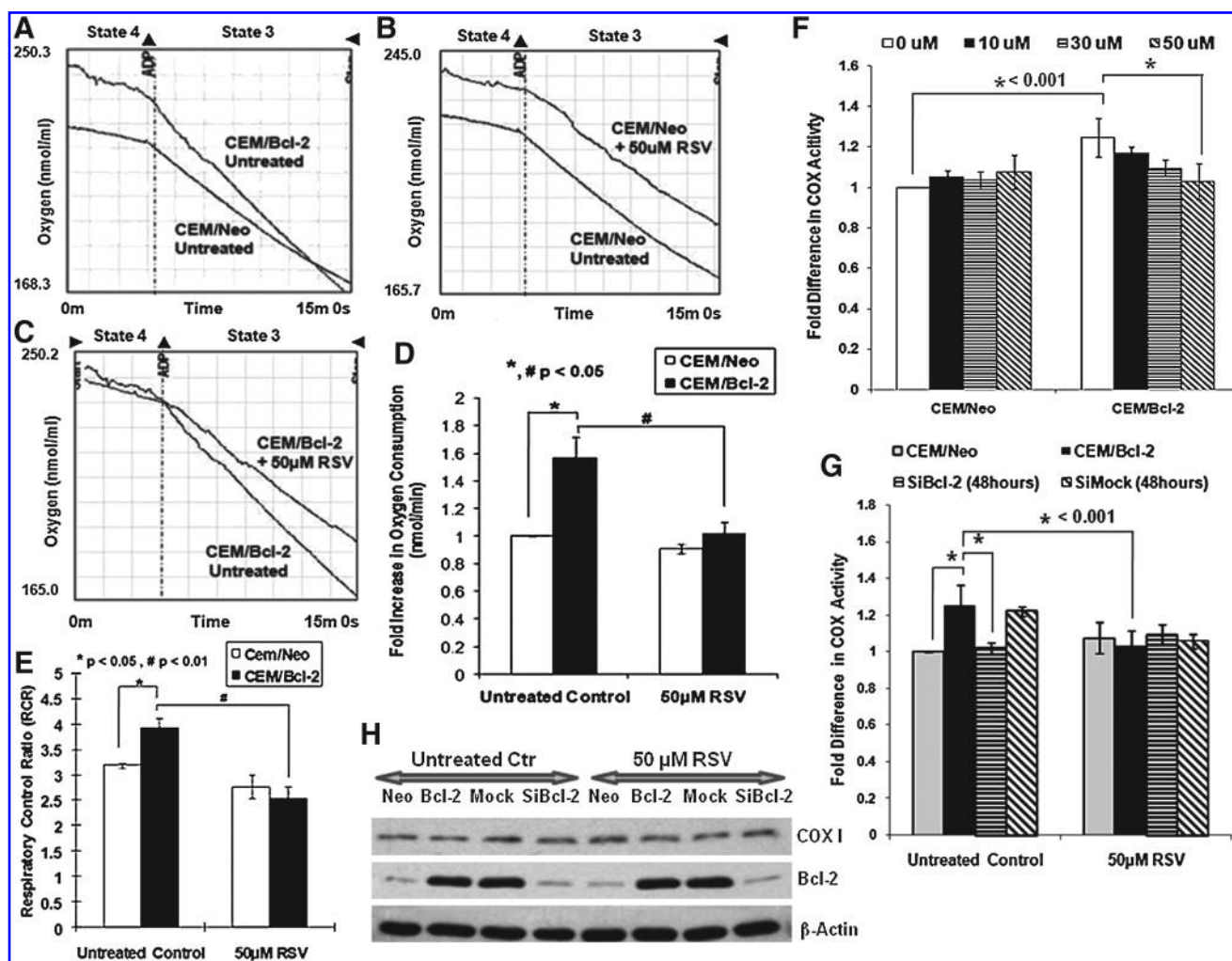


**FIG. 8. RSV slows down mitochondrial oxygen consumption and inhibits COX activity.** (A, B, C, and D) Mitochondrial oxygen consumption was monitored in succinate-respiring mitochondria isolated from CEM/Neo and CEM/Bcl-2 cells following 6 h treatment with 50  $\mu$ M RSV. State 4 respiration was initiated in the presence of ATP, while state 3 respiration was initiated subsequently with 0.2 mM ADP. All samples were normalized prior to the initiation of experiment and reverse electron flow was inhibited with rotenone. (E) Respiratory control ratio (RCR) indicating a tighter coupling in CEM/Bcl-2 than CEM/Neo cells. RCR values ranging from 3 to 10 are typical for oxygen consumption studies using isolated mitochondria. (F) COX activity was measured in CEM/Neo and CEM/Bcl-2 cells using the COX microplate assay kit obtained from Mitosciences (Eugene, OR) as described in Materials and Methods. (G) COX activity was measured after siRNA-mediated downregulation of Bcl-2 in CEM/Bcl-2 cells. siMock represents CEM/Bcl-2 cells transfected with non-scrambled siRNA. Silencing of Bcl-2 was achieved 48 h after the transfection of CEM/Bcl-2 cells with Bcl-2 specific siRNA. Data shown are Mean  $\pm$  SD of at least three independent experiments. (H) Expression level of COX subunit I was analyzed 18 h after RSV treatment by SDS-PAGE and Western blot analysis.

The absence of  $H_2O_2$  production, despite the observed burst in  $O_2^-$  upon RSV treatment, may be seemingly paradoxical, as any increase in mitochondrial  $O_2^-$  level would expectedly bring about a concomitant increase in the conversion of  $O_2^-$  into  $H_2O_2$  by MnSOD. We nevertheless reason that without the upregulation in MnSOD level upon RSV treatment, the increase in mitochondrial  $O_2^-$  induced by RSV would have rapidly saturated the existing MnSOD enzymes. Therefore, any further increase in mitochondrial  $O_2^-$  production would not lead to a corresponding increase in  $H_2O_2$  production. In addition, any minute increase in  $H_2O_2$  production prior to the saturation of MnSOD would be rapidly quenched by the vast plethora of highly efficient  $H_2O_2$  scavengers, such as glutathione perox-

idase, catalase, and peroxiredoxins, residing in the mitochondria. Moreover, expression of MnSOD in CEM cells appears to be considerably lower than that of several other common tumor cell types (data not shown), further justifying the higher propensity for the saturation of MnSOD in our system. In fact, it may be plausible that the observed  $O_2^-$  burst triggered by RSV may be a cell type-dependent phenomenon since a low level of MnSOD may be a necessary criterion for the observed burst in  $O_2^-$  production.

The involvement of Bax and Bak in RSV-induced cell death has remained elusive to date. While several studies have reported the critical role of Bax and Bak in RSV's death-inducing effect (5, 13), others have reported the converse (22, 23).



However, such contradiction could be explained, at least in part, by the difference in MnSOD level of the various cell types being used. In line with this,  $H_2O_2$  has been shown to be critical in the signaling of the mitochondrial translocation of Bax (2), and since cells deficient in MnSOD are unlikely to produce sufficient  $H_2O_2$  upon RSV-treatment, it is not surprising that RSV-induced apoptosis is independent of Bax under such conditions. In fact, our findings provide further insights into an alternative mechanism in which RSV could bypass  $H_2O_2$ -dependent Bax activation via accumulation of mitochondrial  $O_2^-$  to trigger mitochondrial apoptosis.

Unravelling the novel mechanism of Bcl-2 in the regulation of mitochondrial respiration opens up a new chapter in our endeavour to further understand the workings of this anti-apoptotic protein from a noncanonical perspective. By virtue of an increased Bcl-2 expression profile, tumor cells may gain enhanced resilience by fine-tuning their mitochondrial respiration profile to maintain intracellular ROS at a threshold optimal for survival. Under basal conditions, mitochondrial respiration is moderately higher in Bcl-2 overexpressing cancer cells, generating a slight pro-oxidant milieu conducive for tumor maintenance and progression. Conversely, upon the presence of ROS triggers, electron flux across the ETC is reduced to a level sufficient to keep potentially deleterious ROS at bay by controlling the activity of the rate-limiting COX enzyme. In this regard, levels of Bcl-2 expression may be indicative of different tumor sensitivities towards ROS-inducing chemotherapeutics. Thus, an augmented Bcl-2 expression may grant cancer cells with enhanced resistance against ROS-inducing agents, countering the detrimental effects of ROS production via the modulation of mitochondrial respiration. Further elucidation of the regulatory mechanism governing this pathway may potentially reveal new strategies for the sensitization of these resistant tumor cells to ROS-inducing chemotherapeutics as well as other death stimuli.

## Acknowledgments

This work is supported by grants from the National Medical Research Council and the Biomedical Research Council (R-185-000-164-305) of Singapore to S.P.

## Author Disclosure Statement

No competing financial interests exist.

## References

- Adams JM and Cory S. The Bcl-2 apoptotic switch in cancer development and therapy. *Oncogene* 26: 1324–1337, 2007.
- Ahmad KA, Clement MV, Hanif IM, and Pervaiz S. Resveratrol inhibits drug-induced apoptosis in human leukemia cells by creating an intracellular milieu nonpermissive for death execution. *Cancer Res* 64: 1452–1459, 2004.
- Ahmad KA, Clement MV, and Pervaiz S. Pro-oxidant activity of low doses of resveratrol inhibits hydrogen peroxide-induced apoptosis. *Ann NY Acad Sci* 1010: 365–373, 2003.
- Andreyev AY, Kushnareva YE, and Starkov AA. Mitochondrial metabolism of reactive oxygen species. *Biochemistry (Moscow)* 70: 200–214, 2005.
- Aziz MH, Nihal M, Fu VX, Jarrard DF, and Ahmad N. Resveratrol-caused apoptosis of human prostate carcinoma LNCaP cells is mediated via modulation of phosphatidylinositol 3'-kinase/Akt pathway and Bcl-2 family proteins. *Mol Cancer Ther* 5: 1335–1341, 2006.
- Azmi AS, Bhat SH, and Hadi SM. Resveratrol-Cu(II) induced DNA breakage in human peripheral lymphocytes: Implications for anticancer properties. *FEBS Lett* 579: 3131–3135, 2005.
- Azmi AS, Bhat SH, Hanif S, and Hadi SM. Plant polyphenols mobilize endogenous copper in human peripheral lymphocytes leading to oxidative DNA breakage: A putative mechanism for anticancer properties. *FEBS Lett* 580: 533–538, 2006.
- Chen ZX and Pervaiz S. Bcl-2 induces pro-oxidant state by engaging mitochondrial respiration in tumor cells. *Cell Death Differ* 14: 1617–1627, 2007.
- Chen ZX and Pervaiz S. Involvement of cytochrome c oxidase subunits Va and Vb in the regulation of cancer cell metabolism by Bcl-2. *Cell Death Differ* 17: 408–420, 2010.
- Clement MV, Hirpara JL, Chawdhury SH, and Pervaiz S. Chemopreventive agent resveratrol, a natural product derived from grapes, triggers CD95 signaling-dependent apoptosis in human tumor cells. *Blood* 92: 996–1002, 1998.
- Clement MV, Hirpara JL, and Pervaiz S. Decrease in intracellular superoxide sensitizes Bcl-2-overexpressing tumor cells to receptor and drug-induced apoptosis independent of the mitochondria. *Cell Death Differ* 10: 1273–1285, 2003.
- de la Lastra CA and Villegas I. Resveratrol as an anti-inflammatory and anti-aging agent: Mechanisms and clinical implications. *Mol Nutr Food Res* 49: 405–430, 2005.
- Delmas D, Rebe C, Lacour S, Filomenko R, Athias A, Gambert P, Cherkaoui-Malki M, Jannin B, Dubrez-Daloz L, Latruffe N, and Solary E. Resveratrol-induced apoptosis is associated with Fas redistribution in the rafts and the formation of a death-inducing signaling complex in colon cancer cells. *J Biol Chem* 278: 41482–41490, 2003.
- Desole MS, Sciola L, Delogu MR, Sircana S, Migheli R, and Miele E. Role of oxidative stress in the manganese and 1-methyl-4-(2'-ethylphenyl)-1,2,3,6-tetrahydropyridine-induced apoptosis in PC12 cells. *Neurochem Int* 31: 169–176, 1997.
- Fiskum G, Rosenthal RE, Vereczki V, Martin E, Hoffman GE, Chinopoulos C, and Kowaltowski A. Protection against ischemic brain injury by inhibition of mitochondrial oxidative stress. *J Bioenerg Biomemb* 36: 347–352, 2004.
- Frank S, Gaume B, Bergmann-Leitner ES, Leitner WW, Robert EG, Catez F, Smith CL, and Youle RJ. The role of dynamin-related protein 1, a mediator of mitochondrial fission, in apoptosis. *Dev Cell* 1: 515–525, 2001.
- Fukuhara K and Miyata N. Resveratrol as a new type of DNA-cleaving agent. *Bioorg Med Chem Lett* 8: 3187–3192, 1998.
- Janssen YM, Van Houten B, Borm PJ, and Mossman BT. Cell and tissue responses to oxidative damage. *Lab Invest* 69: 261–274, 1993.
- Jiang J, Huang Z, Zhao Q, Feng W, Belikova NA, and Kagan VE. Interplay between bax, reactive oxygen species production, and cardiolipin oxidation during apoptosis. *Biochem Biophys Res Commun* 368: 145–150, 2008.
- Kim R, Emi M, Tanabe K, Murakami S, Uchida Y, and Arihiro K. Regulation and interplay of apoptotic and non-apoptotic cell death. *J Pathol* 208: 319–326, 2006.
- Kopp P. Resveratrol, a phytoestrogen found in red wine. A possible explanation for the conundrum of the 'French paradox'? *Eur J Endocrinol* 138: 619–620, 1998.
- Lee SC, Chan J, Clement MV, and Pervaiz S. Functional proteomics of resveratrol-induced colon cancer cell apoptosis:



- Caspase-6-mediated cleavage of lamin A is a major signaling loop. *Proteomics* 6: 2386–2394, 2006.
23. Mohan J, Gandhi AA, Bhavya BC, Rashmi R, Karunakaran D, Indu R, and Santhoshkumar TR. Caspase-2 triggers Bax-Bak-dependent and -independent cell death in colon cancer cells treated with resveratrol. *J Biol Chem* 281: 17599–17611, 2006.
  24. Mukhopadhyay P, Rajesh M, Yoshihiro K, Hasko G, and Pacher P. Simple quantitative detection of mitochondrial superoxide production in live cells. *Biochem Biophys Res Commun* 358: 203–208, 2007.
  25. Pervaiz S. Resveratrol: From grapevines to mammalian biology. *FASEB J* 17: 1975–1985, 2003.
  26. Pervaiz S and Holme AL. Resveratrol: Its biologic targets and functional activity. *Antioxid Redox Signal* 11: 2851–2897, 2009.
  27. Poh TW and Pervaiz S. LY294002 and LY303511 sensitize tumor cells to drug-induced apoptosis via intracellular hydrogen peroxide production independent of the phosphoinositide 3-kinase-Akt pathway. *Cancer Res* 65: 6264–6274, 2005.
  28. Quinlan T, Spivack S, and Mossman BT. Regulation of antioxidant enzymes in lung after oxidant injury. *Environ Health Perspect* 102 Suppl 2: 79–87, 1994.
  29. Robb EL, Page MM, Wiens BE, and Stuart JA. Molecular mechanisms of oxidative stress resistance induced by resveratrol: Specific and progressive induction of MnSOD. *Biochem Biophys Res Commun* 367: 406–412, 2008.
  30. Robinson BH. The role of manganese superoxide dismutase in health and disease. *J Inherit Metab Dis* 21: 598–603, 1998.
  31. Shenoy K, Wu Y, and Pervaiz S. LY303511 enhances TRAIL sensitivity of SHEP-1 neuroblastoma cells via hydrogen peroxide-mediated mitogen-activated protein kinase activation and up-regulation of death receptors. *Cancer Res* 69: 1941–1950, 2009.
  32. Tinhofer I, Bernhard D, Senfter M, Anether G, Loeffler M, Kroemer G, Kofler R, Csordas A, and Greil R. Resveratrol, a tumor-suppressive compound from grapes, induces apoptosis via a novel mitochondrial pathway controlled by Bcl-2. *FASEB J* 15: 1613–1615, 2001.
  33. Youle RJ and Strasser A. The BCL-2 protein family: Opposing activities that mediate cell death. *Nat Rev Mol Cell Biol* 9: 47–59, 2008.

Address correspondence to:  
 Professor Shazib Pervaiz, M.B.B.S., Ph.D.  
 Department of Physiology  
 Yong Loo Lin School of Medicine  
 National University of Singapore  
 2 Medical Drive, MD9 #01-05  
 Singapore 117597

E-mail: phssp@nus.edu.sg

Date of first submission to ARS Central, December 11, 2009;  
 date of final revised submission, March 2, 2010; date of acceptance, April 1, 2010.

#### Abbreviations Used

COX = cytochrome C oxidase  
 $\Delta\psi_m$  = mitochondrial transmembrane potential:  
 DCHF-DA = dichlorofluorescein diacetate  
 DiOC<sub>6</sub> = 2',7'- 3,3'-dihexyloxycarbocyanine iodide  
 ETC = electron transport chain  
 NAC = N-acetyl cysteine  
 NAO = nonyl acridine orange  
 O<sub>2</sub><sup>-</sup> = reactive oxygen species  
 ROS = superoxide:  
 RSV = resveratrol



**This article has been cited by:**

1. Xi Lin, Gang Wu, Wen-Qian Huo, Yao Zhang, Feng-Shuo Jin. 2012. Resveratrol induces apoptosis associated with mitochondrial dysfunction in bladder carcinoma cells. *International Journal of Urology* **19**:8, 757-764. [[CrossRef](#)]
2. Lalchhandami Tochhawng, Deng Shuo, Shazib Pervaiz, Celestial T. Yap. 2012. Redox regulation of cancer cell migration and invasion. *Mitochondrion* . [[CrossRef](#)]
3. Justyna Mikuś-Pietrasik, Angelika Kuczmarska, Błażej Rubiś, Violetta Filas, Marek Murias, Paweł Zieliński, Katarzyna Piwocka, Krzysztof Księżek. 2012. Resveratrol delays replicative senescence of human mesothelial cells via mobilization of antioxidative and DNA repair mechanisms. *Free Radical Biology and Medicine* **52**:11-12, 2234-2245. [[CrossRef](#)]
4. S. Shrotriya, G. Deep, M. Gu, M. Kaur, A. K. Jain, S. Inturi, R. Agarwal, C. Agarwal. 2012. Generation of reactive oxygen species by grape seed extract causes irreparable DNA damage leading to G2/M arrest and apoptosis selectively in head and neck squamous cell carcinoma cells. *Carcinogenesis* . [[CrossRef](#)]
5. Jia Kang, Shazib Pervaiz. 2012. Mitochondria: Redox Metabolism and Dysfunction. *Biochemistry Research International* **2012**, 1-14. [[CrossRef](#)]
6. Ivan Cherh Chiet Low , Jia Kang , Shazib Pervaiz . 2011. Bcl-2: A Prime Regulator of Mitochondrial Redox Metabolism in Cancer Cells. *Antioxidants & Redox Signaling* **15**:12, 2975-2987. [[Abstract](#)] [[Full Text HTML](#)] [[Full Text PDF](#)] [[Full Text PDF with Links](#)]
7. Zhengguang Wang, Weiping Li, Xiangling Meng, Benli Jia. 2011. Resveratrol induces gastric cancer cell apoptosis via ROS, but independent of sirtuin1. *Clinical and Experimental Pharmacology and Physiology* no-no. [[CrossRef](#)]
8. Zhaofeng Zhang, Ye Ding, Xiaoqian Dai, Junbo Wang, Yong Li. 2011. Epigallocatechin-3-gallate protects pro-inflammatory cytokine induced injuries in insulin-producing cells through the mitochondrial pathway. *European Journal of Pharmacology* . [[CrossRef](#)]
9. Henriette Kauntz, Souad Bousserouel, Francine Gossé, Francis Raul. 2011. Silibinin triggers apoptotic signaling pathways and autophagic survival response in human colon adenocarcinoma cells and their derived metastatic cells. *Apoptosis* . [[CrossRef](#)]
10. Shefali Krishna, Ivan Cherh Chiet Low, Shazib Pervaiz. 2011. Regulation of mitochondrial metabolism: yet another facet in the biology of the oncoprotein Bcl-2. *Biochemical Journal* **435**:3, 545-551. [[CrossRef](#)]
11. Jin Sang Kil, Yong Son, Yong-Kwan Cheong, Nam-Ho Kim, Hee Jong Jeong, Sung Don Kang, Hun-Taeg Chung, Hyun-Ock Pae. 2011. An anticancer/cytotoxic activity of resveratrol is not hampered by its ability to induce the expression of the antioxidant/cytoprotective heme oxygenase-1 in RAW264.7 cells. *Biomedicine & Preventive Nutrition* **1**:2, 146-152. [[CrossRef](#)]